

Supporting information

Electrochromic properties of vertically aligned Ni-doped WO₃ nanostructure films and their application in complementary electrochromic devices

Junling Zhou, Youxiu Wei, Gui Luo, Jianming Zheng, Chunye Xu*
Hefei National Laboratory for Physical Sciences at the Microscale
CAS Key Laboratory of Soft Matter Chemistry
Department of Polymer Science and Engineering
University of Science and Technology of China, Hefei 230026, PR China
*E-mail: chunye@ustc.edu.cn

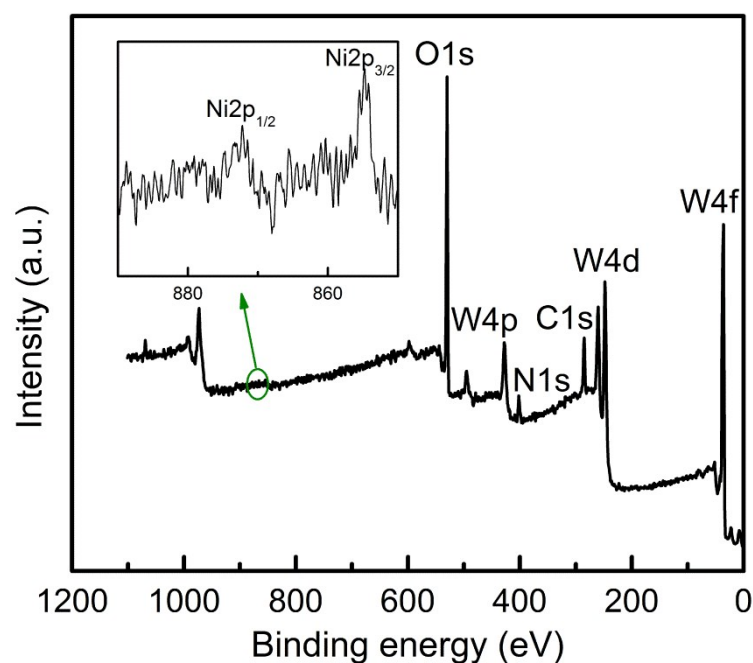


Fig. S1 XPS survey spectra of 2.5% Ni-WO₃ film with inset demonstrating the enlarged view of Ni 2p spectra.

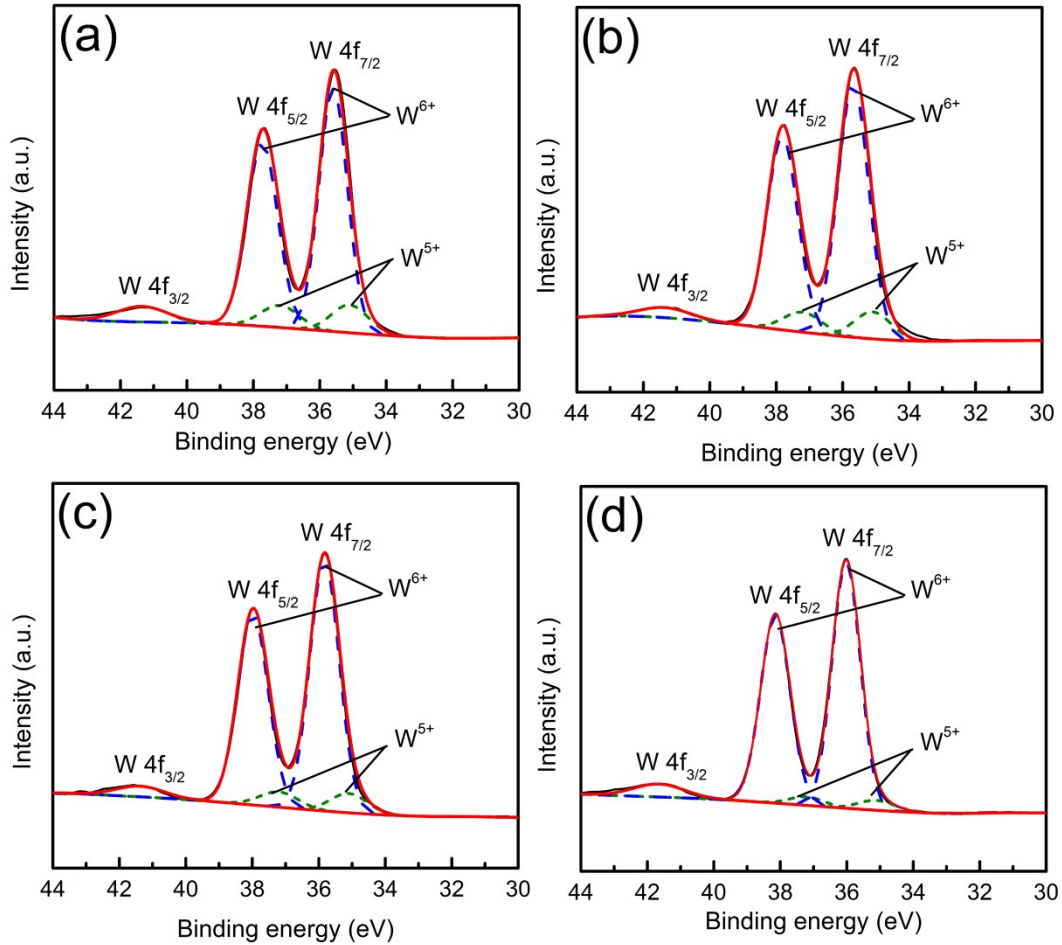


Fig. S2 Fitting peaks of XPS spectra for Ni-WO₃ films with Ni concentration of (a) 0%, (b) 0.5%, (c) 1.5% and (d) 2.5% .

Fig. S3 demonstrates SEM images of WO₃ films with different Ni doping concentration. As shown in Fig. S3 (a), undoped WO₃ film exhibits usual porous and interconnecting network structure composed of nanowires. For 0.5% Ni-WO₃, the surface and cross sectional morphology in Fig. S3 (a) and (h) indicate that most of the nanorods are vertically aligned with increased diameter. For 1%-2% Ni-WO₃, the nanorods are widely arrayed with branches grown around the nanorods. As Ni doping concentration increases, the amount of branches increases and the arrangement of nanorods become denser. When Ni doping concentration increases to 2.5%, nanorods constitute compact surface with nanoflowers composed of nanoplates formed on. For 3% Ni-WO₃, further addition of Ni doping ions induce to smooth and compact surface with thin nanosheets randomly distributed on. In conclusion, for low concentration Ni-WO₃, the arrangement of nanorods becomes wild and dense while more branches grow randomly around the nanorod with increasing Ni doping concentration. For WO₃ with Ni doping concentration higher than 2.5%, nanoplates structure appears and the film become compact as Ni concentration increases.

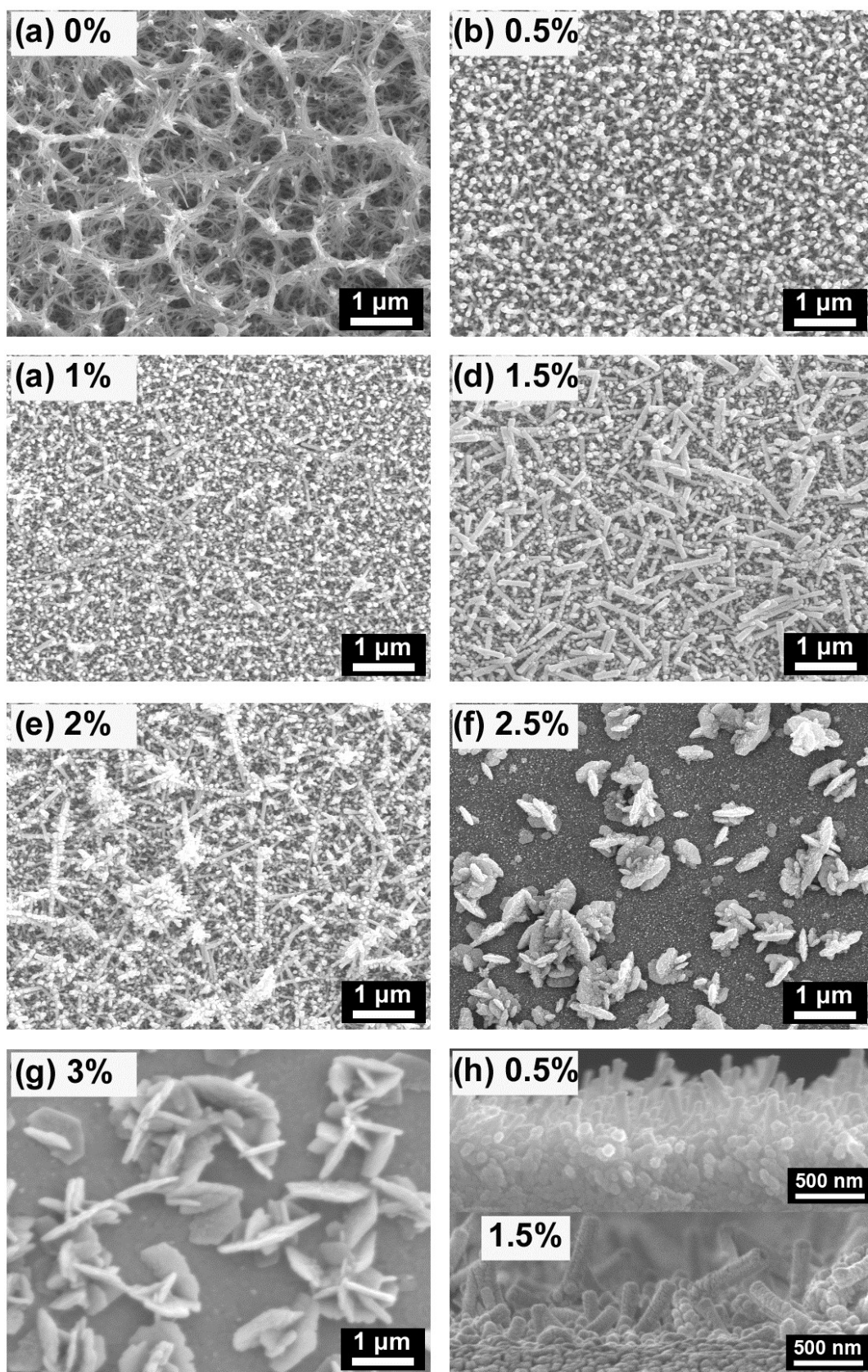


Fig. S3. SEM images of Ni-WO₃ films with Ni doping concentration of 0-3% (a-g) and cross sectional view of 0.5% and 1.5% Ni-WO₃ films (h).

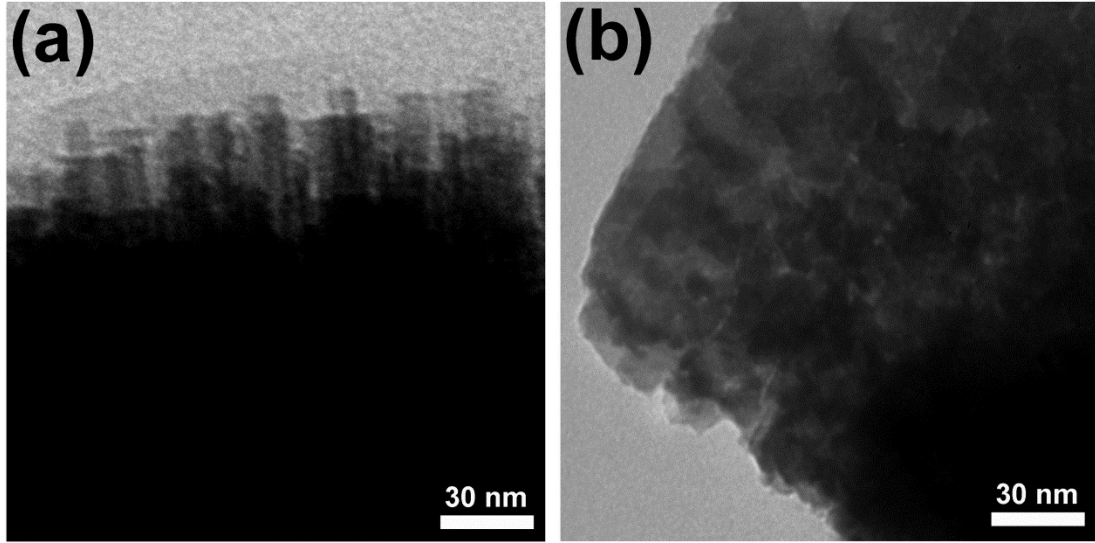


Fig. S4. TEM images of nanorods and nanoplates in 2.5% Ni-WO₃.

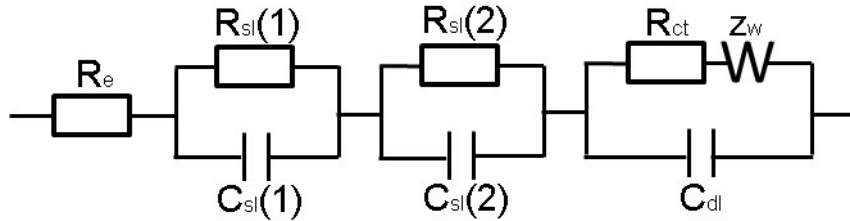


Fig. S5. Equivalent circuit used to fit the experimental EIS data (*Solar energy materials & solar cells*, 2014, **124**, 103-110).

Table S1 Fitting parameters of EIS plots and the calculated conductivity of Ni-WO₃ films.

Ni-WO ₃	R _e (Ω cm ²)	R _{sl} (1) (Ω cm ²)	R _{sl} (2) (Ω cm ²)	R _{ct} (Ω cm ²)	Z _w (S s ^{1/2} cm ⁻²)	Conductivity S/cm
0%	175.1	25.82	33.04	14.57	6.9E-3	4.12E-6
0.5%	178.7	15.46	25.42	9.22	1.9E-3	6.51E-6
1.5%	179.2	30.04	47.62	64.54	4.9E-3	9.30E-7

Fig. S5 presents the equivalent circuit for Ni-WO₃ films with different Ni concentration to simulate the experimental EIS plots. R_e relates to the solution resistance which has no significant difference among the films. R_{sl} (i) and C_{sl} (i) (i=1,2) demonstrates the migration of Li⁺ ions and the capacity of the layer, respectively. R_{ct} and C_{dl} represent the charge transfer resistance and double layer capacitance. Z_w is the Warburg impedance. These parameters can be calculated by Zview software as shown in Table S1. The conductivity represents the electric conductivity through the film which could be calculated from R_{ct} by formula (1) shown below:

$$\sigma = \frac{l}{R_{ct} A} \quad (1)$$

where σ represents the conductivity of the film, l and A are the thickness and area of the film, and R_{ct} is the charge transfer resistance of the film.

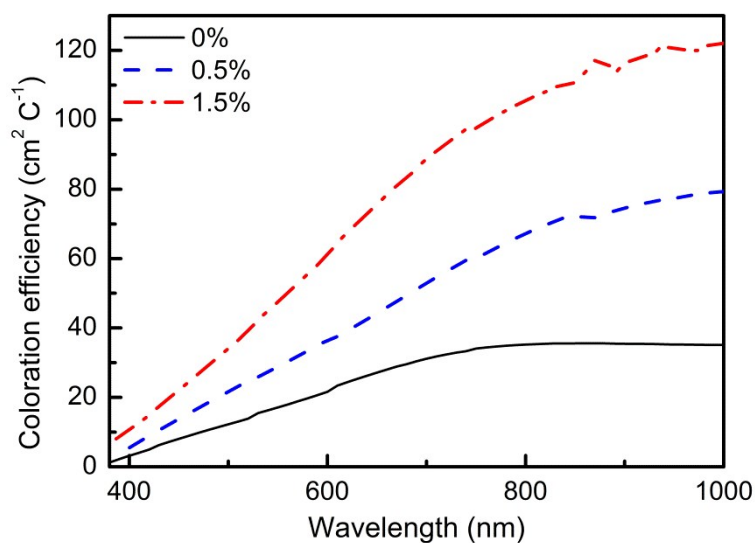


Fig. S6. Spectral coloration efficiency for Ni-WO₃ films with different Ni concentration.

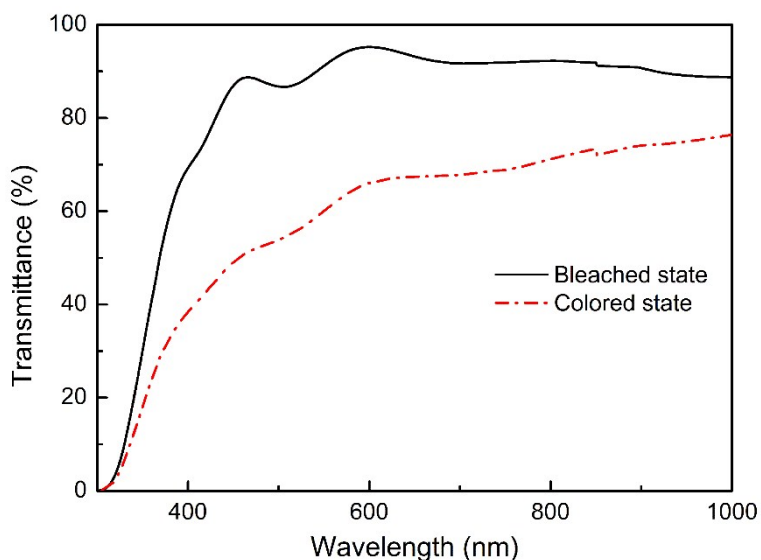


Fig. S7. Transmittance spectra of Li-Ti-NiO films with thickness for about 260 nm.

Fig. S7 illustrates optical properties of Li-Ti-NiO film. The film exhibits excellent optical transmittance for over 70% in visible and near-infrared region at bleached state, and maximum optical modulation of about 38% at 450 nm. The Li-Ti-NiO film shows good optical modulation properties in visible region.

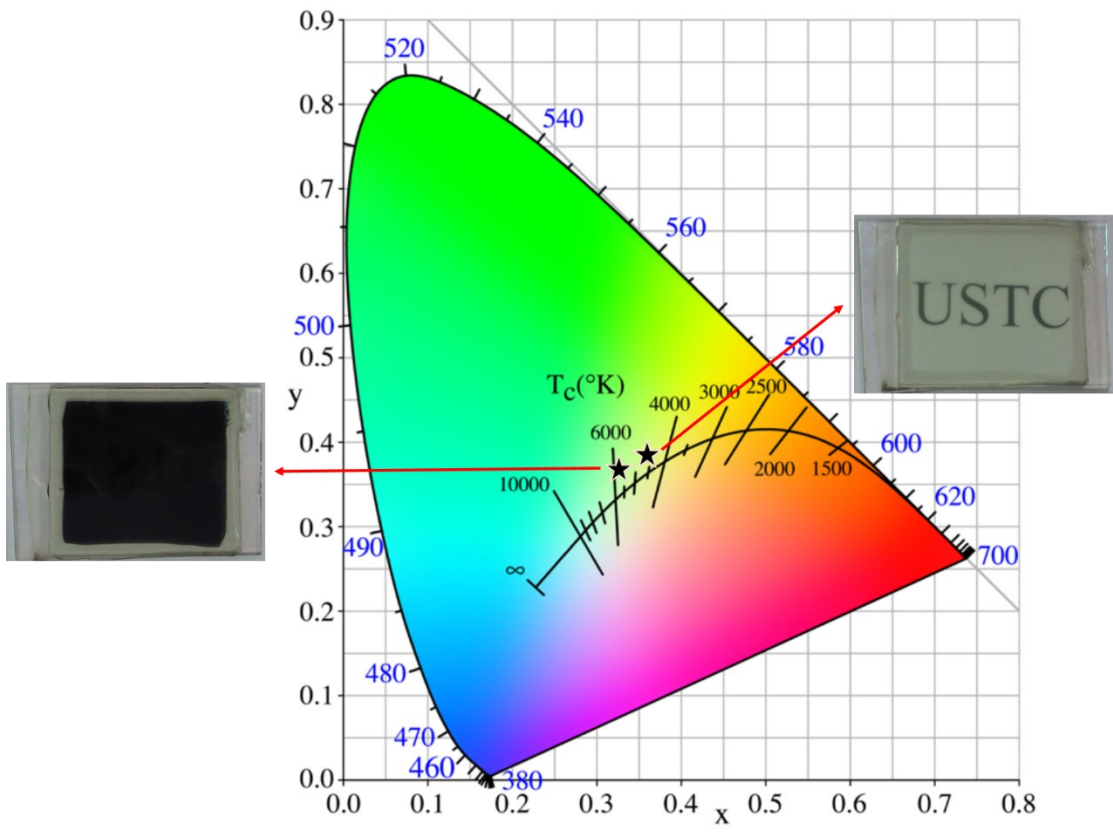


Fig. S8. CIE 1931 color space of liquid ECD in bleached and colored state.